Chemically enhanced CO_2 gas exchange in a eutrophic lake: A general model[1]

Steve Emerson[2]
Lamont-Doherty Geological Observatory of Columbia University, Palisades, New York 10965

Abstract

The exchange of carbon dioxide between the atmosphere and water is governed by the kinetics of diffusion and reaction in the interfacial boundary layer. Previous derivations of the equations describing this process are not always applicable to lakes. A general model, developed to explain the CO_2 exchange rate in eutrophic Lake 227 of the Experimental Lakes Area, indicates that carbon dioxide invasion into this lake is five to ten times that predicted if there were no reaction. The model results conform with data from laboratory CO_2 invasion experiments. The large chemical enchancement in Lake 227 is caused by a strong CO_2 gradient resulting from an epilimnion depleted of carbon dioxide by eutrophication. These results indicate that calculations of the CO_2 gas exchange rate, especially in eutrophic lakes, must consider the possibility of a relatively large enhancement factor.

Two studies of the carbon dioxide invasion rate into artificially eutrophied Lake 227 of the Experimental Lakes Area (Schindler et al. 1972; Emerson et al. 1973) showed that the invasion of CO_2 into this lake could not be explained by assuming a simple diffusion process. To quantify the effect of reactions on the CO_2 gas exchange rate, empirical data were derived from a lake simulation experiment and whole lake carbon mass balance. This study deals with the theoretical basis for the relatively large observed "enhancement factor" and presents a model that can be used to solve the general problem of chemically enhanced gas exchange.

I thank W. S. Broecker for his direction and advice during this research. Discussions with D. Hammond helped clarify some aspects of the enhanced gas exchange process, and S. Ben-Yaakov provided helpful criticism with respect to the problem of ion diffusion.

Background

Chemical data for Lake 227 and details of the eutrophication experiment were given by Schindler and Fee (1974). For background, the important aspects of the data pertaining to the carbon dioxide exchange rate calculations are: the lake water is very low in electrolytes; the ionic strength is roughly 10^{-4} M and the total carbon concentration, $\Sigma CO_2 = HCO_3^- + CO_3^{2-} + CO_{2aq}$, was about 100 μM in 1970—the year for which the calculation is made. The large phytoplankton standing crop brought about by the eutrophication experiment caused the CO_{2aq} concentration in the epilimnion to drop well below atmospheric saturation, resulting in a rise of pH to about 10 in summer. The very low dissolved CO_2 caused a large net influx of atmospheric carbon. To quantify this carbon source an evaluation of the CO_2 exchange rate was necessary.

The gas exchange model used in this study is the Lewis-Whitman stagnant boundary layer. This model assumes a thin stagnant layer of water at the lake–atmosphere interface through which gases and ions travel by molecular diffusion, with the atmosphere above and the epilimnion below assumed to be well mixed. The thickness of the boundary layer depicts the hydrodynamic properties controlling gas exchange. Details of the model and a description of the method by which the boundary layer thickness for Lake 227 was

[1] Contribution of Lamont-Doherty Geological Observatory. This research was supported by U.S. Atomic Energy Commission contracts AT(11-1)3135 and AT(11-1)3180 and National Science Foundation grants GA29459 and GA35103.

[2] Present address: Swiss Federal Institute of Technology (EAWAG), CH-8600 Dübendorf/ZII, Switzerland.

Table 1. Equations governing the three cases of CO_2 gas exchange: A—No enhancement; B—kinetic enhancement; C—equilibrium enhancement.

A—		
	$F_{CO_2} = \frac{D_{CO_2}}{Z} ([CO_2^{atm}] - [CO_2^{o}])$	(1)
B—		
	$D_{CO_2} \frac{d^2[CO_2]}{dx^2} = -r_{CO_2}$	(2)
	$F_t = F_{CO_2} + F_{HCO_3^-} + F_{CO_3^{2-}} = \text{constant}$	(3)
	$O = F_{HCO_3^-} + 2F_{CO_3^{2-}} + F_{OH^-}$	(4)
	$\frac{K_2}{Kw} = \frac{a_{CO_3^{2-}}}{a_{HCO_3^-} a_{OH^-}}$	(5)
	$(\frac{d[C_I]}{dx})_{x=o} = 0; [C_I]_{x=Z} = [C_I^{0}]$	(6)
	$[CO_2]_{x=o} = [CO_2^{atm}]; [CO_2]_{x=Z} = [CO_2^{o}]$	(7)
C—		
	$\frac{K_1}{Kw} = \frac{a_{HCO_3^-}}{a_{CO_2} a_{OH^-}}$	(8)

and Eq. 3-7.

determined to be 600 ± 400 μ are given by Emerson (1975).

The exchange of carbon dioxide across the atmosphere–water interface is determined not only by the physical properties of the water, but also by its reactions with water or OH^- ions during the transport process. The magnitude of chemical enhancement (the true flux divided by the flux predicted if there were no reaction) is determined by the simultaneous kinetics of CO_2 reaction and diffusion in the boundary layer. If reaction and diffusion kinetics are of comparable magnitude, during invasion some of the CO_2 that enters the layer is transformed to HCO_3^-. Because CO_2 is depleted by reaction near the atmosphere–water interface, diffusion into the layer is enhanced. At steady state the total carbon transport everywhere in the layer is the same as that near the interface because of the flux of bicarbonate and carbonate ions.

Theory

The equations governing the transport of carbon species in the boundary layer are given in Table 1. Three different cases are represented. Case A describes the CO_2 flux if there were no reaction; this is the lower limit of carbon dioxide transfer and is approached when the transport of CO_2 through the boundary layer by diffusion is much faster than the kinetics of CO_2 reaction. Equation 1 is Fick's first law where F_{CO_2} and D_{CO_2} are the flux and diffusion coefficient of carbon dioxide, Z is the stagnant boundary layer thickness, and CO_2^{Atm} and CO_2^0 are the carbon dioxide concentrations at the boundary layer interfaces—CO_2^{Atm} is atmospheric saturation and CO_2^0 the concentration in the epilimnion. (Brackets are used to represent concentrations in moles cm^{-3} in the equations.)

If the residence times of CO_2 in the boundary layer with respect to diffusion and reaction are comparable, case B, Eq. 2–7 describe the steady state carbon flux. Equation 2 is the CO_2 conservation equation where x is distance in the layer and r_{CO_2} is the reaction rate of carbon dioxide with water and OH^- ions. At steady state the total carbon flux, F_t, is constant throughout the boundary layer (Eq. 3), and electroneutrality requires that the sum of the fluxes of the reacting ions, HCO_3^-, CO_3^{2-}, and OH^-, equal zero (Eq. 4). Equation 5 is the instantaneous equilibrium represented by the second dissociation constant of carbonic acid, K_2, combined with the ionization product of water, Kw. The transport equations are completed by specifying the appropriate boundary conditions for ions, C_I, and for CO_2 in Eq. 6 and 7. (*See* Quinn and Otto 1971 for a review of Eq. 2–7.)

The upper limit for CO_2 transfer is satisfied if the residence time of carbon dioxide in the boundary layer is long enough for it to achieve equilibrium with bicarbonate. In case C, Eq. 8, which is the equilibrium described by the first dissociation constant of carbonic acid, K_1, and Eq. 3 through 7 govern the gas exchange process. This case is called equilibrium enhancement.

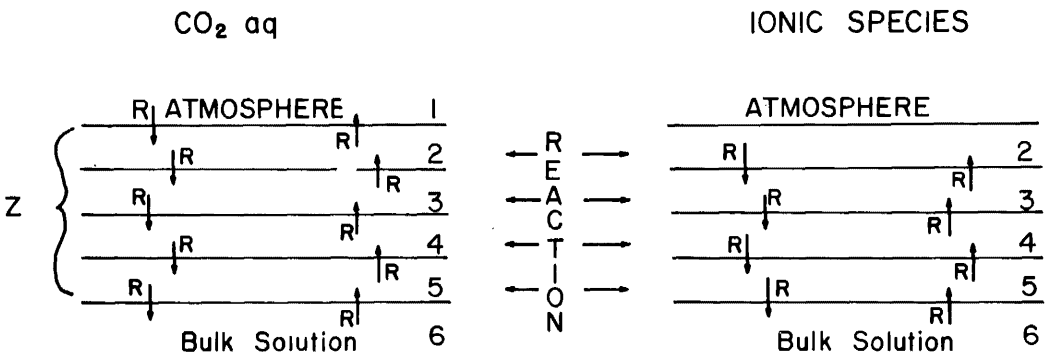

Fig. 1. A schematic representation of the multireservoir diffusion model; Z is the boundary layer thickness, and R is a transfer velocity between reservoirs.

The upper and lower limits of the CO_2 gas exchange rate can be solved fairly simply if the stagnant boundary layer thickness and chemical data are available (*see results*). It is the intermediate case that causes computation difficulties because of the nonlinear reaction term on the right side of Eq. 2.

Shortened forms of Eq. 2 through 7 have been solved for industrial purposes (e.g. Wall 1966; Dankwertz 1970) and for application to oceanic gas exchange (Quinn and Otto 1971). In these cases the bicarbonate-carbonate concentrations overwhelm the hydroxyl ion concentration, hence the third term on the right side of Eq. 4 can be dropped. Since the mobilities of bicarbonate and carbonate ions are roughly the same, this simplification allows one to assume, by the amended form of Eq. 4, that the flux of CO_3^{2-} is in the opposite direction and half that of HCO_3^-. The simple substitution of 4 into 3 follows to provide a more workable set of equations (Quinn and Otto 1971).

A second simplification in the oceanic solution is the assumption that CO_2 reaction with OH^- is unimportant because the pH is about 8. This assumption would be invalid if applied to eutrophic lakes, which in summer usually have surface water pH values between 9 and 10. In this pH region the direct combination of CO_2 with OH^- is the most important reaction pathway (*see* Kern 1960).

The high pH and low alkalinity (Alk = $HCO_3^- + CO_3^{2-} + OH^- = 200$ μeq liter^{-1}) in the surface waters of Lake 227 make previous solutions for the chemically enhanced carbon dioxide exchange rate inadequate. In this case it is unjustified to neglect the role of the OH^- ion in either the CO_2 reaction kinetics or the electroneutrality flux equation. A general solution to the CO_2 transport equations is necessary.

Kinetic enhancement: A numerical model

To solve the problem defined by Eq. 2–7, I define it as a stepwise interaction of a set of nonsteady state ordinary differential equations for diffusion and reaction. The diffusion portion of the model is a graphical representation of a series of equations of the type in Eq. 2 (written in the nonsteady state form) with the reaction term equal to zero and an electroneutrality restriction. The reaction part of the model incorporates the CO_2 reaction kinetics on the right side of Eq. 2 and the equilibria in 5 coupled with ΣCO_2 and charge balance restrictions.

A schematic representation of the model is given in Fig. 1. The boundary layer, Z, is divided into a series of well mixed reservoirs—not necessarily four as shown in the figure. The separation between CO_2 and ionic species is simply to illustrate the difference between the upper boundary condition for CO_2 and ionic diffusion. The problem is solved by starting with an initial condition which defines the CO_2, HCO_3^-, CO_3^{2-}, and OH^- concentrations in the

boundary layer as equal to the equilibrium values in the bulk, i.e. a concentration discontinuity at the atmosphere interface. The boundary conditions require that the CO_2 concentration of layer 1 be held constant—equal to atmospheric saturation—and all concentrations in the bulk remain unchanged. The solution begins by diffusing CO_2 into the layers for a brief period, Δt, during which no reaction occurs. After the diffusion step, the CO_2 concentration in the reservoirs is no longer at equilibrium with bicarbonate, carbonate, and hydroxyl ion. Reaction then occurs for an equal period during which there is no diffusion. Once the reaction step is complete there are gradients in ionic species which then diffuse, for the same Δt, while CO_2 diffusion and reaction are dormant. This cycle is repeated until the concentrations in the well mixed layers come to a steady state. The number of layers was increased and the time interval decreased until further change caused virtually no difference in the results.

Diffusion—Simulation of diffusion by a series of well mixed reservoirs requires the establishment of a transfer velocity R (Fig. 1). This aspect of the model follows a scheme devised by Broecker (1966) to examine the vertical mixing rate in the oceanic thermocline, using the nonsteady state distribution of manmade isotopes. The distribution of a species at any given time in the boundary layer requires the simultaneous solution of a differential mass balance equation, of the type given in Table 2, for each layer. In Eq. 9 C is the concentration per unit volume of the species, the subscript i indicates the layer, and N is the number of layers in Z, excluding those representing the atmosphere and the bulk (or epilimnion).

The calculation of ionic transport is complicated by the charge neutrality restriction and the different ionic mobilities. Vinograd and McBain (1941) and Robinson and Stokes (1970), using the Nernst theory, have shown that the driving force for diffusion of each ion involves both the concentration gradient of that ion and the

Table 2. Equations describing the diffusion of CO_2 and ions in the kinetic enhancement model.

CO_2:

$$\frac{dC_i}{dt} = R_{CO_2}(N/Z)(C_{i-1} + C_{i+1} - 2C_i) \quad (9)$$

$$R_{CO_2} = D_{CO_2}(N+2/Z) \quad (10)$$

Ions:

interface i-1:i

$$\frac{Z}{N+1}\frac{dC}{dt} = R_{ion}(C_{i-1} - C_i)$$

interface i:i+1

$$\frac{Z}{N+1}\frac{dC}{dt} = R_{ion}(C_{i+1} - C_i) \quad (12)$$

$$R_{ion} = D_{ion}(N+1/Z)$$

$$\frac{dC_{ij}}{dt} = R_{ion}(N+1/Z)[C_{i-1}+C_{i+1}-2C_i]_j - z_j\left[(C_{i-1}+C_i)_j \frac{\sum_k u_k z_k (C_{i-1}-C_i)_k}{\sum_k u_k z_k^2 (C_{i-1}+C_i)_k} + (C_{i+1}+C_i)_j \frac{\sum_k u_k z_k (C_{i+1}-C_i)_k}{\sum_k u_k z_k^2 (C_{i+1}+C_i)_k}\right] \quad (13)$$

gradient of electrical potential in the solution. Imposing the constraint of electroneutrality they derive an equation for the flux of each ion, F_j, in terms of its mobility, u, charge, z, concentration gradient, dC/dx, and these properties for all ions, k, in solution. Ben-Yaakov (1972) investigated this effect on the transport of ions in seawater. His equation 4 expressed in my terms is

$$F_j = RTu_j\left[\frac{dC_j}{dx} - C_j z_j \frac{\sum_k u_k z_k dC_k/dx}{\sum_k u_k z_k^2 C_k}\right]. \quad (11)$$

All concentrations, C, are in moles cm^{-3}, RT is the gas constant times absolute temperature, and the product RTu_j is the value of the true diffusion coefficient of the ion under no influence of a potential gradient.

Ben-Yaakov (1972) showed that the electrical potential term (second term on the right side of 11) does not cause a large effect with respect to the diffusion of ions in interstitial waters of marine sediments. In the case here, however, the diffusing ions are a large portion of the total charge

Table 3. Equations describing the kinetics of CO_2 reactions in the kinetic enhancement model.

$$\Sigma CO_2 = [HCO_3^-] + [CO_3^{2-}] + [CO_2] \quad (14)$$

$$\sum_m n[C_m^{n+}] - \sum_m n[A_m^{n-}] = Alk = [HCO_3^-] + 2[CO_3^{2-}] + [OH^-] \quad (15)$$

$$\frac{d[CO_2]}{dt} = -(k_1 + k_3[OH^-])[CO_2] + (k_{-1}Kw/[OH^-] + k_{-3})[HCO_3^-] \quad (16)$$

CO_2:

$$\frac{d[CO_2]}{dt} = -\{k_1 + k_3[OH^-] + 2k_{-1}(Kw/[OH^-] + 2k_{-3}\}[CO_2] + 2\Sigma CO_2\{k_1(Kw/[OH^-]) + k_{-3}\} - Alk\{k_{-1}(Kw/[OH^-]) + k_{-3}\} + k_{-1}Kw + k_{-3}[OH^-] \quad (17)$$

OH^-:

$$[HCO_3^-] = 1/2(Alk - 2\Sigma CO_2 + 2[CO_2] + Kw/K_2) + 1/2\,(Alk - 2\Sigma CO_2 + 2[CO_2] + Kw/K_2)^2 + 4Kw/K_2(\Sigma CO_2 - [CO_2])^{1/2} \quad (18)$$

$$[OH^-] = (Kw/K_2)(\Sigma CO_2 - [HCO_3^-] - [CO_2])/[HCO_3^-] \quad (19)$$

in solution and their mobilities range by a factor of five (*see Table 5*). The use of a simple diffusion equation of the type in 9 for the ionic fluxes is unjustified.

To incorporate this process into the diffusion model, Eq. 9 can be rewritten in terms of fluxes across the interfaces which bound each layer as in Eq. 12. These equations are then combined with 11 by assuming linear gradients and average concentrations (*see* Sherwood and Wei 1955) and then summed to form Eq. 13. All ions, including those which do not take part in reactions, are subject to the constraint in 13.

The simultaneous differential equations were solved by a predictor-corrector method (McCracken and Dorn 1967). The value of dt in Eq. 9 and 13 was decreased until further reduction caused no significant difference in the diffusion kinetics. A value of 0.02 s satisfactorily met this criterion.

Reaction—After CO_2 diffusion the chemistry in the boundary layer is in a state of nonequilibrium. The concentrations which sufficiently define the state in each layer are the new ΣCO_2 and the alkalinity (Eq. 14 and 15: Table 3). In 15 the summations are for all, m, cations, C, and anions, A, with valences, n, which do not take part in the CO_2 reactions.

The rate at which the carbonate chemistry in the layers tends toward a new equilibrium is given in Eq. 16 (Kern 1960). k_1 and k_{-1} are the forward and reverse rate constants of CO_2 reaction with water; k_3 and k_{-3} are these rate constants with respect to CO_2 reaction with OH^- ions. By combining Eq. 14, 15, and 16 into 17, the reaction rate of CO_2 is written in terms of known constants, OH^-, CO_2, Alk, and ΣCO_2. This equation is solved for each layer, using new values of CO_2 and ΣCO_2, resulting from carbon dioxide diffusion, and Alk and OH^- concentrations that are a result of the initial conditions or the previous ion diffusion step.

Since Eq. 17 represents second order kinetics—CO_2 and OH^- are both consumed during the reaction—a time (dt) brief enough so that there is only a small change in CO_2 and OH^- is chosen. After dt the OH^- concentration is readjusted by 18 and 19 which are a combination of the Alk, ΣCO_2, and K_2 equilibria. The new OH^- and CO_2 are substituted back into 17 and the procedure is repeated.

The rate equation was solved by the same method used in the diffusion scheme. A time interval, dt, of 0.02 s successfully simulated the second order chemical reaction.

Table 4. A flow chart outlining the sequence of reaction and diffusion in the kinetic enhancement model; Δt is the length of time between alternation of reaction and diffusion.

	Initial Conditions
	a. $[HCO_3^-]$, $[CO_3^{2-}]$, $[OH^-]$, $\sum_m[C_m^{n+}]$ and $\sum_m[A_m^{n-}]$ in all the layers equal the bulk concentrations
	↓
Δt	b. CO_2 in atmosphere reservoir = $[CO_2^{atm}]$
	CO_2 in bulk reservoir = $[CO_2^{o}]$
	↓
0.1 s	Diffuse CO_2
	Solve N+2 simultaneous equations of the type in 9 for five 0.02-s intervals (dt = 0.02 s)
	↓
	Recalculate ΣCO_2 in all layers
	↓
0.1 s	Reaction in each layer
	Solve N equations of the type in 17 recalculating the OH^- concentration by 18&19 every 0.02 s (dt = 0.02 s)
	↓
0.1 s	Diffuse ions
	For each ion solve N+1 simultaneous equations of the type in 13 for five 0.02-s intervals
	↓
	Recalculate Alk in all layers

Table 4 is a flow chart outlining the organization of the procedure used to solve the complete problem. Reduction of the time between alternation of diffusion and reaction from 0.1 to 0.05 s resulted in less than a 2% difference in the end results. The solutions came to steady state after about 100 s for a stagnant boundary layer of 300 μ and 500 s for a layer of 1,000 μ. There was virtually no change in the steady state result on increasing the number of layers beyond 15; for the calculation I use $N = 20$.

Calculation results

Table 5 presents the data used in the calculations. To reduce the number of equations necessary for the diffusion calculation, species not involved in the reaction are expressed as an average cation AC^{2+} and an

Table 5. Data used in the enhancement factor calculations. A—Ionic concentrations (see Armstrong and Schindler 1971) and equivalent conductances, λ^o (Robinson and Stokes 1970); in Eq. 20 F is Faraday's constant (96,500 Ceq^{-1}) and u the mobility (cm^2 mole J^{-1} s^{-1}). B—Equilibrium and rate constants for the carbonate system.

A—

Species	λ^o (mho $cm^2 eq^{-1}$)	C (eq $cm^{-3} \times 10^{+9}$)
Ca^{2+}	60	85
Mg^{2+}	53	85
Na^+	50	90
SO_4^{2-}	80	60
CO_3^{2-}	69	50
HCO_3^-	44	55
OH^-	198	95
AC^{2+*}	71	260
$AA^{2-\dagger}$	80	60

$$u_i = \frac{\lambda^o}{|z_i| F^2} \qquad (20)$$

B—

Constant (pure water, 25°C)	Reference
$K_1 = 4.45 \times 10^{-7}$	Harnard and Davis (1943)
$K_2 = 4.68 \times 10^{-8}$	Harnard and Davis (1943)
$Kw = 1.0 \times 10^{-14}$	Robinson and Stokes (1970)
$k_1 = 0.03\ s^{-1}$	Kern (1960)
$k_3 = 8500\ M^{-1} s^{-1}$	Kern (1960)

*AC^{2+} = average cations = $Ca^{2+} + Mg^{2+} + Na^+$

$$\lambda^o_{AC^{2+}} = \frac{\lambda^o Ca^{2+} + \lambda^o Mg^{2+} + 2\lambda^o Na^+}{3}.$$

†AA^{2-} = average anion = SO_4^{2-}.

Table 6. Results of the CO_2 gas exchange calculations. A—No enhancement; B—kinetic enhancement; C—equilibrium enhancement.

Case	z (μ)	Invasion rate ($m\ m^{-2} s^{-1} \times 10^{+12}$)	Enhancement factor
A (Lake 227)	300	7.0	
	600	3.5	
	1,000	2.1	
B (Lake 227)	300	37	5
	600	30	9
	1,000	21	10
C (Lake 227)	300	150	21
	600	75	21
	1,000	43	21
B (simulation experiment)	400	19	3.6

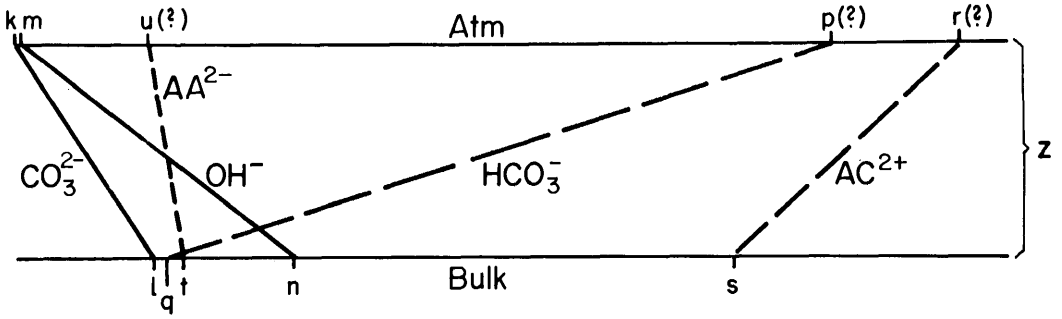

Fig. 2. Species gradients across the Lake 227 boundary layer at chemical equilibrium. Concentrations are given in Table 5 and calculation procedures in Table 7 (the lower boundary values are relative concentrations in equivalents).

average anion AA^{2-}. In Lake 227 AC^{2+} is about a third each Ca^{2+}, Mg^{2+}, and Na^+; AA^{2-} is almost entirely SO_4^{2-}. The mobility of a species can be calculated from equivalence conductance, λ^0, data by Eq. 20. Equilibrium constants used here are for pure water and 25°C; this is justified by the very low dissolved ion concentration in the lake water. The best approximation for species concentrations is that they equal activities.

Table 7. The procedure for solving equilibrium enhancement. A—Species gradients, invasion is negative. B—The three equations governing the atmosphere–water boundary values of AC^{2+}, AA^{2-}, *and* HCO_3^- *(see Fig. 2 and Sherwood and Wei 1955).*

A—

Species	Gradient (dC_i/dx) $(m\ cm^{-4})$	C_i $(m\ cm^{-3})$
HCO_3^-	$-\frac{p-q}{z}$	$\frac{q+p}{2}$
OH^-	$\frac{n}{z}$	$\frac{n}{2}$
CO_3^{2-}	$\frac{L}{z}$	$\frac{L}{2}$
AC^{2+}	$-\frac{r-s}{z}$	$\frac{r+s}{2}$
AA^{2-}	$\frac{t-u}{z}$	$\frac{u+t}{2}$

B—

$$2r = (p + 2u)_{x=0} \qquad (21)$$

$$0 = -(r-130\times10^{-9})-2(r+130\times10^{-9}) \times \left[\frac{-71r+44p+80u-16\times10^{-6}}{142r+44p+160u+48\times10^{-6}}\right] \qquad (22)$$

$$0 = (30\times10^{-9}-u)+2(u+30\times10^{-9}) \times \left[\frac{-71r+44p+80u-16\times10^{-6}}{142r+44p+160u+48\times10^{-6}}\right] \qquad (23)$$

$p = 400 \times 10^{-9}\ m\ cm^{-3}$
$u = 18 \times 10^{-9}\ m\ cm^{-3}$
$r = 218 \times 10^{-9}\ m\ cm^{-3}$

The CO_2 invasion rate was calculated for the three cases represented in Table 1. The results, as a function of boundary layer thickness, are given in Table 6. The difference between the lower limit—no enhancement—and the upper limit—equilibrium enhancement—is about 21. The reason for this enormous theoretical enhancement factor maximum is clarified by Fig. 2, which shows the species gradients to be expected if the boundary layer is at chemical equilibrium. The assumption is made here that the OH^- and CO_3^{2-} concentrations in equilibrium with atmospheric CO_2 are negligible compared to their epilimnion values. This assumption is good if the alkalinity at the atmosphere–water interface remains below about 500 μeq liter^{-1}.

At steady state the fluxes of the average cation and average anion are zero. The gradient thus formed in these species must exactly balance the charge potential created by the OH^- ion diffusing against HCO_3^- and with CO_3^{2-}. Since the mobility of hydroxyl ion is about five times that of bicarbonate and carbonate, the result is to create an excess negative charge near the atmosphere–water interface. Cations thus migrate to the interface and anions away.

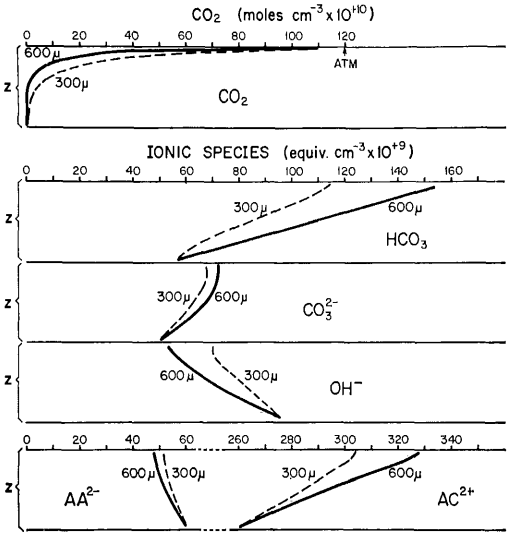

Fig. 3. Concentration profiles of different species across the stagnant boundary layer of Lake 227. The profiles represent steady state results of the model calculations for 300 and 600 μ.

Two equations of the type in 11 plus electroneutrality are sufficient to derive the atmosphere–water boundary concentrations of HCO_3^-, AA^{2-}, and AC^{2+} (Table 7). These values are then used in the HCO_3^- and CO_3^{2-} flux equations to calculate equilibrium CO_2 transport.

The gradient in alkalinity ($AC^{2+} - AA^{2-}$) as a result of the charge potential is about 200 μeq liter^{-1}. This gradient creates a very large potential enhancement and is further indication that the Nernst flux equations are necessary to the solution of the kinetic problem.

Three solutions to the kinetic problem for Lake 227 conditions are given in Table 6. The steady state gradients generated across boundary layers of 300 and 600 μ are plotted in Fig. 3. The enhancement factor ranges from 5 for 300 μ to 10 for 1,000 μ. The kinetic solution is clearly not near equilibrium. The carbonate ion is diffusing into the lake instead of out. This is a result of the difference in the OH^- and HCO_3^- mobilities and the instantaneous equilibrium governed by Eq. 5. Since the hydroxyl ion diffuses faster, its steady state gradient across the boundary layer is smaller than that of bicarbonate and, because of the potential gradients, the alkalinity increases near the atmosphere–water interface. The K_2 equilibrium is then satisfied by an increase in carbonate in this region. For boundary layers greater than 1,000 μ the time available for CO_2 reaction would eventually increase to the point where enough OH^- would be consumed near the atmosphere interface to decrease the carbonate concentration below its epilimnion value at this boundary.

Even though the OH^- concentration near the atmosphere–water interface is reinforced by its relatively large mobility, the fact that it decreases is another reason for the large boundary layer required for equilibrium. Wall (1966) showed that an increase in CO_2 concentration gradient decreased the enhancement factor during absorption by causing a more rapid depletion of hydroxyl ion near the liquid–air interface, hence slowing the CO_2 reaction rate.

Experimentally determined enhancement factors

To evaluate the ability of the numerical procedure to predict enhancement factors, I did experiments in which the chemistry and gas exchange properties were close to those of Lake 227. The technique and apparatus for these experiments were the same as those used by Peng (1973) and Emerson et al. (1973). Since the methods have been explained previously, I will be brief.

A small tank (60-cm diameter) of turbulent water with a known chemistry provided the basic physical layout for measuring enhancement factors. The physical properties of the water that determine the stagnant boundary layer were simulated by adjusting the rate at which water in the tank was recirculated by a pump. The variation of the mass transfer coefficient with recirculation rate was monitored by the evasion of radon-222 and invasion of atmospheric O_2. Radon evasion rates were established by methods identical to those used to determine the stagnant boundary

layer thickness in lakes. To determine the boundary layer value by O_2 invasion, I first flushed the tank water with helium, purging dissolved oxygen. The ensuing invasion of atmospheric O_2 was monitored with an oxygen meter.

Once the appropriate physical conditions were established, the alkalinity of the initially distilled water was fixed by adding KOH. In the cases described below, enough KOH was added to bring the pH to about 10. The subsequent invasion of atmospheric CO_2 was followed by measuring the increase in ΣCO_2 of the water with a gas chromatograph. The ΣCO_2 measurements are believed to be good to within about 10%. The boundary layer thickness, in this range, is good only to $\pm 100\ \mu$. The boundary layer values determined by the radon method were acquired separately from the actual invasion experiments. Boundary layer thicknesses for the circulation rate used during CO_2 invasion were calculated from the data in Table 8.

The invasion of CO_2 and O_2 were measured simultaneously. Table 8 also shows the increase in O_2 and ΣCO_2 in the initial portion of the experiments where the ΣCO_2 increase with time was most linear. This portion of the experiment is used so that the chemical properties of the tank water which determine CO_2 enhancement (pH and ΣCO_2) match as closely as possible the situation in the lake. Enhancement factors were estimated by dividing the measured CO_2 influx by the invasion rate calculated from the experimentally determined boundary layer values. Table 8 includes the critical parameters for the calculation and the enhancement factors.

Before comparing the experimental results with the model, we should examine a little more closely the degree to which the experiment simulates the natural situation. To do this, we must consider the major differences between the two: The alkalinity in the simulation experiment is about half that of the lake because initially the only species in the tank are potassium and hydroxyl ions. The second important difference is that the bulk ΣCO_2 is constant in the lake but increases in the experiment. Both of these effects cause a smaller enhancement than would be expected for the natural situation. The second effect is the most important and is illustrated by the increase in HCO_3^-, calculated from ΣCO_2 and Alk, with time in Table 8. The bicar-

Table 8. Results of the simulation experiment. A—^{222}Rn-^{226}Ra data. B—The increase in ΣCO_2 and O_2 with time. C—Parameters used to derive enhancement factors.

A—

Rn (cpm	Ra liter^{-1})	Ra:Rn	h* (cm)	Z (μ)
7	305	44	5.0	300
8	254	32	5.0	410
6	256	43	5.0	300

B—

Exp SP-4 Alk = 120 μeq liter^{-1}

Δt (min)	O_2 (ppm)	ΣCO_2 (μM)	$[HCO_3^-]$† (μM)	pH†	h (cm)
0	4.8				
12	5.6	17	12	10.0	
20	5.9				
50	6.4				
65	6.7	36	27	9.9	
180	8.0	65	54	9.7	4.6
310	8.7	82	73	9.5	4.6

Exp SP-5 Alk = 100 μeq liter^{-1}

0	3.6	11			5.0
25	4.4	18	13	9.9	
55	5.1				
70	5.4	29	22	9.8	
100	6.3				5.2
130	6.4				
146	6.7				
178	7.0	57-69	55	9.5	5.2
217	7.3				
280	7.6	86	80	9.2	5.1

C—

Exp	h (cm)	Z_{Rn}‡ (μ)	Z_{O_2}§
SP-4	4.7	300-410	335-400
SP-5	5.1	300-410	500

Exp	Calc. flux (m cm^{-2} s^{-1} × 10+12)	Meas. flux	Enh factor
SP-4	4.8 - 5.7	20.9	3.7 - 4.4
SP-5	3.5 - 5.5	22.7	4.1 - 6.5

*Depth of the water in the tank.

†pH and HCO_3^- calculated from ΣCO_2 and Alk.

‡$=D_{Rn}/(Ra:Rn - 1)\ \lambda_{Rn} h$, where $\lambda_{Rn}=2.1 \times 10^{-6}$ s^{-1}, $D_{Rn}= 1.4 \times 10^{-5} cm^2 s^{-1}$.

§$=(D_{O_2} \Delta t/h)\ \ln(O_2^{atm}-O_2)(O_2^{atm}-O_2^0)^{-1}$, where $O_2^{atm}= 9$ ppm; $O_2^0=$ initial O_2 concn; $D_{O_2}= 2.5 \times 10^{-5} cm^2 s^{-1}$.

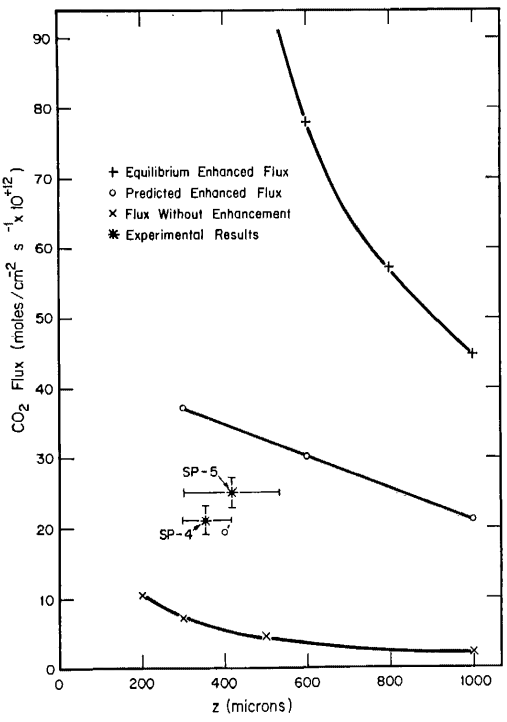

Fig. 4.. CO_2 flux as a function of boundary layer thickness showing calculated results for the three different cases and the experimental results. *O'* is the model result solved for the chemistry of the simulation experiment.

bonate increase during the initial stages of the experiment is nearly as rapid as the ΣCO_2 increase. Thus, the HCO_3^- gradient across the boundary layer is smaller as the experiment progresses—the enhancement factor decreases with time. Consequently, the experiment represents an average enhancement factor for a bulk pH of between 9.2 and 10. This is a minimum value for the case in Lake 227, where the pH is constant at about 10 in summer.

Because the experiment represents only a lower limit for Lake 227 enhancement, a check on the degree of accordance between the model and the empirical results was made by solving the kinetic enhancement factor problem for conditions in Table 8 (Alk = 110 μeq liter^{-1}, mean bulk pH = 9.5, and $Z = 400$ μ). This solution is presented in Table 6; considering the average pH approximation and experimental error, it is in good agreement with the results of Table 8.

Discussion and summary

Figure 4 is a summary of the CO_2 flux as a function of stagnant boundary layer thickness for the cases of no enhancement, equilibrium enhancement, and the model and experimental results. The model results indicate that the enhancement factor increases with increased boundary layer thickness but the total flux decreases. The experimental results agree with the model calculation.

The model predicts that the CO_2 enhancement factor for Lake 227 is between 5 and 10 resulting in an invasion rate of 25 ± 7 mmoles m^{-2} day^{-1} for summer 1970. Schindler et al. (1972) determined the carbon invasion rate in Lake 227 by nutrient balance for the same time period. Their results indicated that 16 ± 4 mmoles of CO_2 invaded each square meter per day. The theoretical and empirical results overlap only for relatively large values of the stagnant boundary layer, suggesting that this range most accurately characterizes the gas exchange rate at that time.

The possibility for catalyzed CO_2 reaction rates in natural waters was suggested by Berger and Libby (1969). The effect of the presence of a catalyst (e.g. carbonic anhydrase) would push the reaction kinetics toward equilibrium and result in a maximum enhancement. A comparison of the model results with those of Schindler et al. indicates that this catalysis is not occurring in Lake 227. For a boundary layer of 600–1,000 μ the equilibrium invasion rate would be 50 ± 15 mmoles m^{-2} day^{-1}, well above the experimental error in carbon balance calculation.

Lake 227 represents a rather extreme case for enhanced CO_2 gas exchange because of its relatively large stagnant boundary layer (*see* Emerson 1975), low ionic concentration, and high pH. The factors controlling carbon dioxide gas transfer in most natural waters will lie somewhere between those of Lake 227 and the ocean

(*see* Quinn and Otto 1971). There is, thus, a wide range of physical and chemical conditions between the two cases that have been studied.

Here I demonstrated the procedures for calculating the CO_2 exchange rate. To estimate the minimum flux only the boundary layer thickness and CO_2 concentration need be known. A maximum can be determined if additional information about the carbonate chemistry is available. If the capacity for CO_2 enhancement is great, the range between the lower and upper limiting exchange rates may be as large as an order of magnitude, as in Lake 227.

To determine the intermediate case, one must calculate the steady state carbon flux from the kinetics of CO_2 reaction and diffusion. Because of the wide range of alkalinity and pH of natural waters, simplified derivations of the enhancement factor used for the ocean are not always applicable. The model presented here is general and could be applied to many physical and chemical situations.

References

ARMSTRONG, F. A. J., AND D. W. SCHINDLER. 1971. Preliminary chemical characterization of waters in the Experimental Lakes Area, northwestern Ontario. J. Fish. Res. Bd. Can. **28**: 171–187.

BEN-YAAKOV, S. 1972. Diffusion of sea water ions–1. Diffusion of seawater into a dilute solution. Geochim. Cosmochim. Acta **36**: 1395–1406.

BERGER, R., AND W. F. LIBBY. 1969. Equilibration of atmospheric carbon dioxide with sea water: Possible enzymatic control rate. Science **164**: 1395–1397.

BROECKER, W. S. 1966. Radioisotopes and the rate of mixing across the main thermocline of the ocean. J. Geophys. Res. **71**: 5827–5836.

DANKWERTZ, P. V. 1970. Gas-liquid reactions. McGraw-Hill.

EMERSON, S. 1975. Gas exchange rates in small Canadian Shield lakes. Limnol. Oceanogr. **20**: 754–761.

———, W. S. BROECKER, AND D. W. SCHINDLER. 1973. Gas exchange rates in a small lake as determined by the radon method. J. Fish. Res. Bd. Can. **30**: 1475–1484.

HARNARD, H. S., AND R. DAVIS. 1943. The ionization constant of carbonic acid in water and the solubility of CO_2 in water and aqueous salt solution from 0° to 50°C. J. Am. Chem. Soc. **65**: 2030.

KERN, D. M. 1960. The hydration of carbon dioxide. J. Chem. Educ. **37**: 14–23.

MCCRACKEN, D. D., AND W. S. DORN. 1967. Numerical methods and Fortran programming. Wiley.

PENG, T.-H. 1973. Determination of gas exchange rates across sea–air interface by the radon method. Ph.D. thesis, Columbia Univ.

QUINN, J. A., AND N. C. OTTO. 1971. Carbon dioxide exchange at the air–sea interface: Flux augmentation by chemical reaction. J. Geophys. Res. **76**: 1539–1549.

ROBINSON, R. A., AND R. H. STOKES. 1970. Electrolyte solutions. Butterworths.

SCHINDLER, D. W., G. J. BRUNSKILL, S. EMERSON, W. S. BROECKER, AND T.-H. PENG. 1972. Atmospheric carbon dioxide: Its role in determining phytoplankton standing crops. Science **177**: 1192–1194.

———, AND E. J. FEE. 1974. Experimental Lakes Area: Whole-lake experiments in eutrophication. J. Fish. Res. Bd. Can. **31**: 937–953.

SHERWOOD, T. K., AND J. C. WEI. 1955. Diffusion in mass transfer between phases. Am. Inst. Chem. Eng. **1**: 522–527.

VINOGRAD, J. R., AND J. W. MCBAIN. 1941. Diffusion of electrolytes and of ions in their mixtures. J. Am. Chem. Soc. **63**: 2008–2015.

WALL, H. H. 1966. Absorption and desorption of carbon dioxide in carbonate-bicarbonate solutions. M.S. thesis, Univ. Delaware.

Submitted: 8 July 1974
Accepted: 24 April 1975